

# London penetration depth and superfluid density of single-crystalline $\text{Fe}_{1+y}(\text{Te}_{1-x}\text{Se}_x)$ and $\text{Fe}_{1+y}(\text{Te}_{1-x}\text{S}_x)$

H. Kim,<sup>1</sup> C. Martin,<sup>1,\*</sup> R. T. Gordon,<sup>1</sup> M. A. Tanatar,<sup>1</sup> J. Hu,<sup>2</sup> B. Qian,<sup>2</sup> Z. Q. Mao,<sup>2</sup> Rongwei Hu,<sup>3,†</sup> C. Petrovic,<sup>3</sup> N. Salovich,<sup>4</sup> R. Giannetta,<sup>4</sup> and R. Prozorov<sup>1,‡</sup>

<sup>1</sup>Ames Laboratory and Department of Physics & Astronomy, Iowa State University, Ames, Iowa 50011, USA

<sup>2</sup>Department of Physics and Engineering Physics, Tulane University, New Orleans, Louisiana 70118, USA

<sup>3</sup>Condensed Matter Physics and Materials Science Department, Brookhaven National Laboratory, Upton, New York 11973, USA

<sup>4</sup>Loomis Laboratory of Physics, University of Illinois at Urbana-Champaign, Urbana, Illinois 61801, USA

(Received 12 January 2010; revised manuscript received 13 March 2010; published 10 May 2010)

The in-plane London penetration depth,  $\lambda(T)$ , was measured in single crystals of the iron-chalcogenide superconductors  $\text{Fe}_{1.03}(\text{Te}_{0.63}\text{Se}_{0.37})$  and  $\text{Fe}_{1.06}(\text{Te}_{0.88}\text{S}_{0.14})$  by using a radio-frequency tunnel diode resonator. Similar to the iron-arsenides and in stark contrast to the iron-phosphides, iron-chalcogenides exhibit a nearly quadratic temperature variation of  $\lambda(T)$  at low temperatures. The absolute value of the penetration depth in the  $T \rightarrow 0$  limit was determined for  $\text{Fe}_{1.03}(\text{Te}_{0.63}\text{Se}_{0.37})$  by using an Al coating technique, giving  $\lambda(0) \approx 560 \pm 20$  nm. The superfluid density  $\rho_s(T) = \lambda^2(0)/\lambda^2(T)$  was fitted with a self-consistent two-gap  $\gamma$  model. While two different gaps are needed to describe the full-range temperature variation in  $\rho_s(T)$ , a nonexponential low-temperature behavior requires pair-breaking scattering, and therefore an unconventional (e.g.,  $s_{\pm}$  or nodal) order parameter.

DOI: 10.1103/PhysRevB.81.180503

PACS number(s): 74.70.Xa, 74.25.N-, 74.20.Mn, 74.20.Rp

The majority of Fe-based superconductors are pnictides.<sup>1,2</sup> The only exception so far are the binary iron-chalcogenides  $\text{Fe}_{1+y}(\text{Te},\text{Se})$  and  $\text{Fe}_{1+y}(\text{Te},\text{S})$ , with the excess Fe occupying interstitial site of the chalcogen layers.<sup>3,4</sup> In these “11” materials Fe forms square planar sheets whereas chalcogen ions form distorted tetrahedra surrounding the Fe ions, which is similar to the structure of the Fe-pnictides. The electronic structure of iron-chalcogenides is also similar to pnictides. For the “11” system it has been suggested both theoretically<sup>5</sup> and experimentally<sup>6</sup> that superconductivity could be magnetically mediated. Furthermore, the series of iron-chalcogenides from FeS through FeTe was theoretically explored within the spin-fluctuation picture, concluding that doped FeTe could exhibit the strongest superconductivity.<sup>5</sup> The systems over which the doping is most controlled are  $\text{FeTe}_{1-x}\text{Se}_x$  (Ref. 7) and  $\text{FeTe}_{1-x}\text{S}_x$ .<sup>8</sup> So far the highest  $T_c \approx 15$  K is reported for the  $\text{Fe}(\text{Te},\text{Se})$  system.<sup>7,9</sup> The connection between superconductivity and magnetism in the “11” system has been demonstrated by the observation of the antiferromagnetic order in  $\text{Fe}_{1+y}\text{Te}$  (Ref. 4) and a spin resonance in  $\text{Fe}_{1+y}(\text{Te}_{0.6}\text{Se}_{0.4})$ .<sup>10</sup>  $\text{Fe}(\text{Te},\text{S})$  is a superconductor with  $T_c \approx 8.8$  K and its comprehensive characterization is described in Ref. 11. The transition temperature of FeSe can be enhanced up to 37 K by applying modest pressures,<sup>12</sup> which is comparable to the  $T_c$  of iron arsenides. This connection between  $T_c$  and the pressure has been suggested to come from the enhancement of spin fluctuations<sup>13</sup> and from the modulation of electronic properties due to evolution of the interlayer Se-Fe-Se separations.<sup>12</sup> Several experimental works have explored the pairing mechanism of the “11” compounds.<sup>14–16</sup> The absence of a coherence peak in NMR measurements on polycrystalline FeSe suggests unconventional superconductivity<sup>14</sup> while the power-law temperature dependence of the spin-relaxation rate,  $1/T_1 \sim T^3$ , could be reconciled with both a nodal gap or a fully gapped  $s_{\pm}$  state. Muon spin rotation studies of the penetration depth in  $\text{FeSe}_x$  is consistent with either anisotropic  $s$ -wave or a two-gap ex-

tended  $s$ -wave pairing.<sup>15</sup> Thermal conductivity measurements concluded multigap nodeless superconductivity in polycrystalline  $\text{FeSe}_x$ .<sup>16</sup>

The London penetration depth in iron chalcogenides are very important in view of nonuniversal behavior of different Fe-based families. While in most iron arsenides the measurements of the in-plane penetration depth reveal weak temperature dependence, inconsistent with line nodes in the superconducting gap,<sup>17–24</sup> in phosphorus and phosphorus-containing  $\text{LaPFeO}$  (Ref. 25) and  $\text{BaFe}_2(\text{As}_{1-x}\text{P}_x)_2$  (Ref. 26) the results are compatible with nodal superconductivity.

In this work, we present an experimental study of the in-plane London penetration depth,  $\lambda(T)$ , in single crystals of  $\text{Fe}(\text{Te},\text{Se})$  and  $\text{Fe}(\text{Te},\text{S})$ . We found that at low temperatures  $\Delta\lambda(T) \propto T^n$  with  $n \approx 2.1$  for  $\text{Fe}(\text{Te},\text{Se})$  and  $n \approx 1.8$  for  $\text{Fe}(\text{Te},\text{S})$ . The absolute value of  $\lambda(0) \approx 560$  nm was determined for  $\text{Fe}(\text{Te},\text{Se})$  by measuring the total  $\lambda(T)$  of the sample coated with a thin Al film.<sup>27</sup> The in-plane superfluid density  $\rho_s(T) = \lambda^2(0)/\lambda^2(T)$  was analyzed in the framework of a self-consistent two-gap  $\gamma$  model.<sup>28</sup>

Single crystals of  $\text{Fe}(\text{Te},\text{Se})$  were synthesized using a flux method. Mixed powders of the  $\text{Fe}(\text{Te}_{0.6}\text{Se}_{0.4})$  compositions were sealed in evacuated quartz tubes. The sealed ampoule was slowly heated up to 930 °C and slowly cooled down to 400 °C at a rate of 3 °C/hr before the furnace was shut down. Single crystals with centimeter dimensions can easily be obtained with this method and are shown to be the pure  $\alpha$  phase with the  $P4/nmm$  space group by x-ray diffraction.<sup>9</sup> Single crystals of  $\text{Fe}(\text{Te},\text{S})$  were grown from  $\text{TeS}$  self-flux using a high-temperature flux method. Elemental Fe, Te, and S were sealed in quartz tubes under a partial argon atmosphere. The sealed ampoule was heated to a soaking temperature of 430–450 °C for 24 h, followed by a rapid heating to the growth temperature at 850 °C and then slowly cooled to 820 °C. The excess flux was removed from the crystals by decanting. X-ray diffraction studies indicated high quality of the crystals.<sup>11</sup> The compositions of the

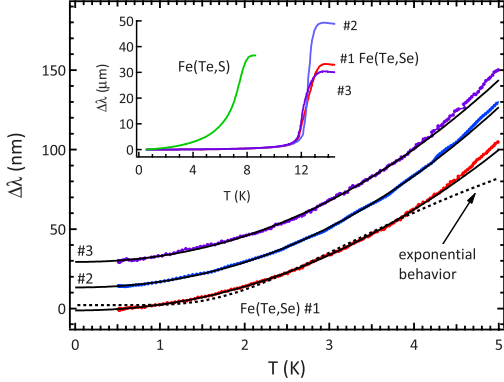


FIG. 1. (Color online) Main panel: variation in the London penetration depth,  $\Delta\lambda(T)$  for three Fe(Te,Se) samples in the low temperature range shown along with the fitting curves assuming power-law or *s*-wave BCS behavior. The curves for samples #2 and #3 of Fe(Te,Se) are shifted vertically for clarity by 15 and 30 nm, respectively. Inset:  $\Delta\lambda(T)$  for three Fe(Te,Se) samples and one Fe(Te,S) sample.

samples used in this work,  $\text{Fe}_{1.03}(\text{Te}_{0.63}\text{Se}_{0.37})$  and  $\text{Fe}_{1.06(3)}(\text{Te}_{0.88(1)}\text{S}_{0.14(2)})$ , were measured by an energy dispersive x-ray spectroscopy.

The in-plane London penetration depth,  $\lambda(T)$ , was measured by using a self-oscillating tunnel-diode resonator.<sup>29–31</sup> The sample was mounted on a sapphire rod which was inserted into a tank-circuit inductor. The weak ac magnetic field  $H_{\text{ac}} \sim 20$  mOe produced by the coil was much smaller than the lower critical field  $H_{c1} < 100$  Oe, so the sample was in the Meissner state, and its magnetic response was determined by the London penetration depth. To probe the *ab*-plane supercurrent response, the sample was placed with its crystallographic *c*-axis along  $H_{\text{ac}}$ . The shift of the resonance frequency,  $\Delta f \equiv f(T) - f_0$ , is measured to obtain the total magnetic susceptibility  $\chi(T)$  via  $\Delta f = -G4\pi\chi(T)$ . Here  $f_0 \approx 14$  MHz is the resonance frequency of an empty resonator,  $G = f_0 V_s / 2V_c(1-N)$  is the calibration factor that depends on the demagnetization factor  $N$ , sample volume  $V_s$ , and coil volume  $V_c$ . The calibration factor is determined for each sample by measuring the full frequency change resulting from physically pulling the sample out of the coil at the lowest temperature. In the Meissner state the magnetic susceptibility,  $4\pi\chi$ , can be written in terms of  $\lambda$  and the effective sample dimension  $R$  as:  $4\pi\chi = (\lambda/R)\tanh(R/\lambda) - 1$ , from which  $\lambda$  can be obtained.<sup>30</sup>

The inset in Fig. 1 shows the full-temperature range penetration depth for Fe(Te,Se) and Fe(Te,S) superconductors. The “maximum slope,”  $T_c^{\text{slope}}$ , determined by taking the maximum of the derivative  $d\Delta\lambda(T)/dT$  gives  $T_c^{\text{slope}} \approx 12.0$  K for Fe(Te,Se) and  $T_c^{\text{slope}} \approx 7.5$  K for Fe(Te,S) while the “onset” values,  $T_c^{\text{onset}} \approx 13$  K for Fe(Te,Se) and  $T_c^{\text{onset}} \approx 8$  K for Fe(Te,S). The low-temperature variation in  $\lambda(T)$  is examined in the main panel of Fig. 1. The dashed line represents the best fit to a standard *s*-wave BCS function,  $\Delta\lambda(T) = \lambda(0)\sqrt{\pi\Delta_0/2T} \exp(-\Delta_0/T)$ , with  $\lambda(0)$  and  $\Delta_0$  being free fitting parameters. The experimental data do not show any indication of saturation down to  $0.04T_c$ , and the fit is not adequate. Also obtained from the fit value of  $\Delta_0 = 0.5T_c$  is impossible in a single-gap scenario. We discuss the multigap

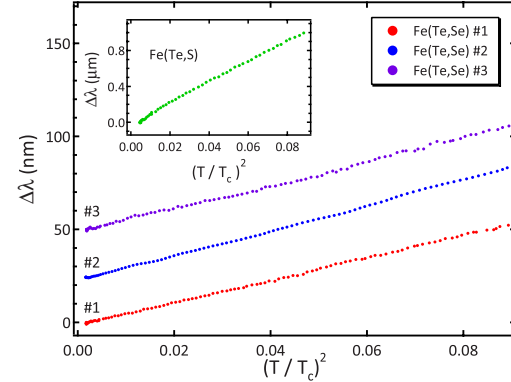


FIG. 2. (Color online)  $\Delta\lambda$  plotted vs.  $(T/T_c)^2$  for three Fe(Te,Se) crystals in the main panel and Fe(Te,S) crystal in the inset in the temperature range up to  $T_c/3$ . The curves for Fe(Te,Se), samples #2 and #3, are shifted vertically by 50 and 25 nm, respectively.

scenario latter. On the other hand, fitting with the power law,  $\Delta\lambda(T) \propto AT^n$ ,  $n = 2.10 \pm 0.01$ , produces excellent agreement with the data.

In order to examine how close the overall power-law variation is to quadratic, we plot  $\Delta\lambda$  versus  $(T/T_c)^2$  for Fe(Te,Se) in the main panel of Fig. 2 and for Fe(Te,S) in the inset. All samples follow the  $\Delta\lambda(T) \propto T^2$  behavior rather well. To probe how robust the power  $n$  is we performed a data fit over a floating temperature range, from  $T=0$  to  $T_{\text{up}}$ , using a functional form of  $\Delta\lambda(T) = a_0 + AT^n$ . The difference between the  $a_0$  term determined from an extrapolation of the  $T^2$  plot in Fig. 2 and from the power-law fit turned out to be negligible,  $1.5 \pm 0.5$  nm, and had no significant effect on the fit. The dependence of the other fitting parameters,  $n$  and  $A$ , on  $T_{\text{up}}$  (selected in the range from  $T_c/6$  to  $T_c/3$ ) is summarized in Fig. 3. The upper panel of Fig. 3 shows the exponent  $n$ , which (1) does not depend much on the selection of the upper limit of the fitting range and (2) is somewhat smaller in Fe(Te,S),  $n \approx 1.8$ , than in Fe(Te,Se),  $n \approx 2$ . The prefactor  $A$  obtained from the fit does not depend much on the fitting range either (indeed, the variation in  $A$ , shown by the dashed lines, is larger because  $n$  was also a free variable).

To calculate the superfluid density, we need to know the absolute value of the penetration depth,  $\lambda(0)$ . We used the technique described in Ref. 27. A thin aluminum layer was deposited using magnetron sputtering conducted in an argon atmosphere. The Al-layer thickness,  $t = 100 \pm 10$  nm, was determined by using an Inficon XTC 2 with a 6 MHz gold quartz crystal and later directly measured by using scanning electron microscopy on the trench made by a focused ion beam. By measuring the frequency shift from  $T \ll T_c^{\text{Al}}$  to  $T > T_c^{\text{Al}}$  and converting it into the effective penetration depth of the coated sample,  $\lambda_{\text{eff}}$ , one can extract the full penetration depth of the material under study from

$$\lambda_{\text{eff}} = \lambda_{\text{Al}} \frac{\lambda + \lambda_{\text{Al}} \tanh(t/\lambda_{\text{Al}})}{\lambda_{\text{Al}} + \lambda \tanh(t/\lambda_{\text{Al}})}, \quad (1)$$

where  $\lambda$  is the unknown penetration depth to be determined. Figure 4 shows the measured  $\lambda_{\text{eff}}(T)$  that is compared to the data without Al coating. The negative offset of  $t - \lambda_{\text{Al}}(0)$

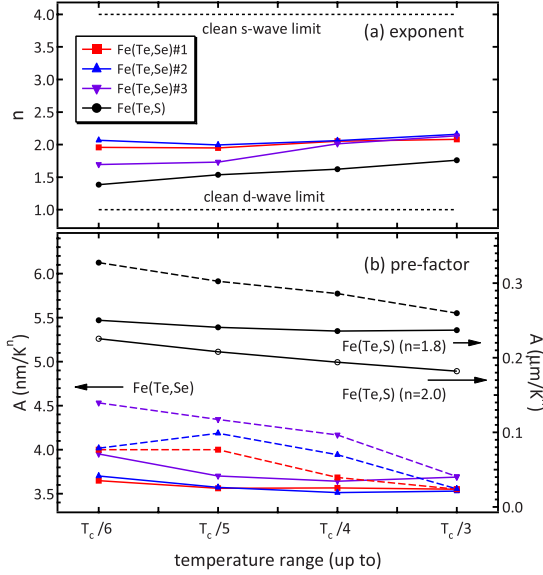


FIG. 3. (Color online) Exponent  $n$  and prefactor  $A$  obtained by fitting to  $\Delta\lambda(T) \propto AT^n$  for various upper temperature limits shown on the  $x$  axis. The exponents in the upper panel were obtained with  $n$  and  $A$  both being free parameters. In the lower panel, symbols show  $A$  acquired with a fixed  $n$ , while the dashed lines shows  $A$  obtained when  $n$  was a free parameter as well.

$=0.05$   $\mu\text{m}$  accounts for the thickness,  $t$ , and  $\lambda_{\text{Al}}(0)$  of the Al layer. Solving Eq. (1) for  $\lambda(T_c^{\text{Al}})$  and extrapolating the obtained  $\lambda(T)$  to  $T=0$  gives an estimate of  $\lambda(0) \approx 560 \pm 20$  nm for the penetration depth of Fe(Fe,Se). More details on the method can be found in Ref. 27.

The superfluid density,  $\rho_s(T) = \lambda^2(0)/\lambda^2(T)$ , shown in Fig. 5, exhibits a noticeable positive curvature at elevated temperatures, similar to MgB<sub>2</sub>.<sup>32</sup> This suggests a multigap superconductivity, which we analyze in the framework of the self-consistent  $\gamma$  model.<sup>28</sup> Of course, this clean  $s$ -wave model should not work at the lowest temperatures, where we observe the power-law behavior in Figs. 1 and 2. It still provides a reasonable description at the intermediated temperatures where thermal excitations dominate scattering and gap anisotropy. Fitting in the temperature range from  $0.45T_c$

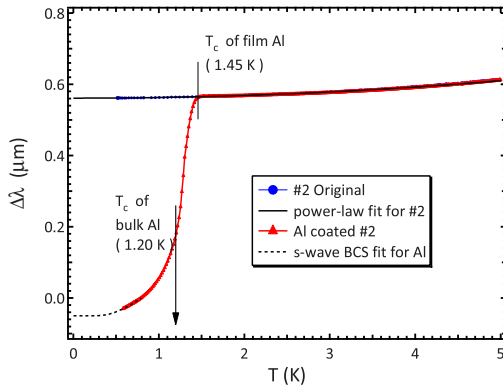


FIG. 4. (Color online) Effective penetration depth in single crystal Fe(Fe,Se) before (blue circles) and after (red triangles) coating with an Al layer. The curve is shifted up according to Eq. (1) and the data are extrapolated to  $T=0$  using a  $T^2$  fit resulting in  $\lambda(0) \approx 560 \pm 20$  nm.

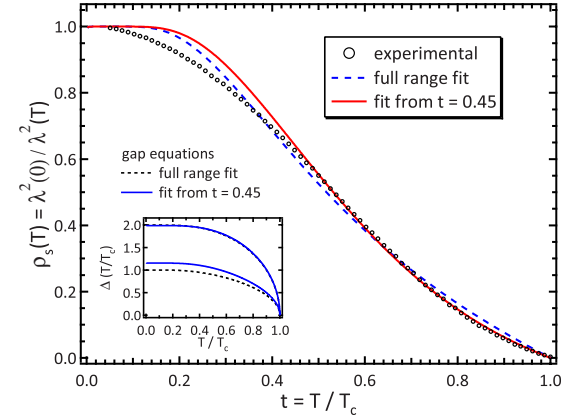


FIG. 5. (Color online) Superfluid density  $\rho_s(T/T_c)$  for Fe(Fe,Se) calculated with experimental  $\Delta\lambda(T)$  and  $\lambda(0)=560$  nm. The solid (red) line is a fit to the two-gap  $\gamma$  model from  $0.45T_c$  to  $T_c$ . The dashed (blue) line is the fit over the full temperature range. Inset: temperature-dependent superconducting gaps calculated self-consistently during the fitting.

to  $T_c$ , shown by a solid (red) line in Fig. 5, produces a good agreement with the data. To limit the number of the fitting parameters, the partial densities of states were chosen to be equal on the two bands,  $n_1=0.5$ , and the first intraband coupling parameter,  $\lambda_1=0.6$ , was chosen to produce a correct  $T_c \approx 12$  K assuming a Debye temperature of 230 K.<sup>11</sup> (The uncertainty in knowing  $\lambda_1$  does not affect the fit quality or the relative ratios of the fitting parameters.) The parameters obtained in the fit are:  $\lambda_2=0.394$ ,  $\lambda_{12}=0.128$ , and  $\gamma=0$ . This result means that  $\rho_s(T)$  at temperatures of the order of  $T_c$  is fully described by only one component, determined by the band with a smaller gap. The existence of the larger gap and small interband coupling,  $\lambda_{12}$ , are needed, however, to maintain a high  $T_c$ . The fit over the entire temperature range reveals a clear deviation from this clean exponential model at low temperatures. The new fitting parameters of  $\lambda_2=0.315$ ,  $\lambda_{12}=0.152$ , and  $\gamma=0.157$  are close to the previous set, albeit with small, but finite  $\gamma$  indicating 16% contribution of the larger gap to the total superfluid density. The temperature-dependent gaps obtained self-consistently in the fitting are shown in the inset to Fig. 5. While the fitted positive curvature and reasonable coupling parameters indicate a multigap nature of superconductivity in “11” iron-chalcogenide superconductors, the failure at the low temperatures and apparently nonexponential behavior requires an unconventional order parameter (nodal or  $s_{\pm}$ ) with pair-breaking scattering.<sup>24</sup>

In conclusion, a robust power-law behavior of the low-temperature London penetration depth,  $\lambda(T) \propto T^n$  is found in single crystals of  $\text{Fe}_{1.03}(\text{Te}_{0.63}\text{Se}_{0.37})$  and  $\text{Fe}_{1.06(3)}(\text{Te}_{0.88(1)}\text{S}_{0.14(2)})$  with exponent  $n \approx 2.1$  and  $\approx 1.8$ , respectively. For Fe(Fe,Se), the absolute value,  $\lambda(0) \approx 560 \pm 20$  nm, was determined by the coating technique. The analysis of the superfluid density shows a clear signature of multigap superconductivity and a failure of the clean limit  $s$ -wave pairing. Strong scattering can explain our results, but for nonmagnetic scattering centers, nodal or  $s_{\pm}$  pairing is required. Together with other published results, the  $s_{\pm}$  pairing seems to be the best candidate to explain our data.

We thank V. G. Kogan for helpful discussions. Work at

the Ames Laboratory was supported by the division of Materials Science and Engineering, Basic Energy Sciences, Department of Energy (USDOE), under Contract No. DEAC02-07CH11358. The work at Tulane was supported by the NSF under Grant No. DMR-0645305. The work at UIUC was supported by the Center for Emergent Superconductivity, an Energy Frontier Research Center funded by the USDOE Office of Science, Basic Energy Sciences under

Award Number DE-AC0298CH1088. Work at the Brookhaven National Laboratory, which is operated for the USDOE by Brookhaven Science Associates Grant No. DE-AC02-98CH10886, was in part supported by the USDOE Office of Science, Office of Basic Energy Services as part of the Energy Frontier Research Center (EFRC), Center for Emergent Superconductivity (CES). R.P. acknowledges support from the Alfred P. Sloan Foundation.

\*Present address: Department of Physics, University of Florida, Gainesville, FL 32611.

†Present address: Ames Laboratory, Iowa State University, Ames, IA 50011.

‡Corresponding author; prozorov@ameslab.gov

<sup>1</sup>Y. Kamihara, H. Hiramatsu, M. Hirano, R. Kawamura, H. Yanagi, T. Kamiya, and H. Hosono, *J. Am. Chem. Soc.* **128**, 10012 (2006).

<sup>2</sup>Y. Kamihara, T. Watanabe, M. Hirano, and H. Hosono, *J. Am. Chem. Soc.* **130**, 3296 (2008).

<sup>3</sup>F.-C. Hsu, J.-Y. Luo, K.-W. Yeh, T. Chen, T.-W. Huang, P. M. Wu, Y.-C. Lee, Y.-L. Huang, Y.-Y. Chu, D.-C. Yan, and M.-K. Wu, *Proc. Natl. Acad. Sci. U.S.A.* **105**, 14262 (2008).

<sup>4</sup>W. Bao, Y. Qiu, Q. Huang, M. A. Green, P. Zajdel, M. R. Fitzsimmons, M. Zhernenkov, S. Chang, M. Fang, B. Qian, E. K. Vehstedt, J. Yang, H. M. Pham, L. Spinu, and Z. Q. Mao, *Phys. Rev. Lett.* **102**, 247001 (2009).

<sup>5</sup>A. Subedi, L. Zhang, D. J. Singh, and M. H. Du, *Phys. Rev. B* **78**, 134514 (2008).

<sup>6</sup>T.-L. Xia, D. Hou, S. C. Zhao, A. M. Zhang, G. F. Chen, J. L. Luo, N. L. Wang, J. H. Wei, Z.-Y. Lu, and Q. M. Zhang, *Phys. Rev. B* **79**, 140510(R) (2009).

<sup>7</sup>K.-W. Yeh, T.-W. Huang, Y.-L. Huang, T.-K. Chen, F.-Ch. Hsu, Ph. M. Wu, Y.-Ch. Lee, Y.-Y. Chu, Ch.-L. Chen, J.-Y. Luo, D.-Ch. Yan, and M.-K. Wu, *EPL* **84**, 37002 (2008).

<sup>8</sup>Y. Mizuguchi, F. Tomioka, S. Tsuda, T. Yamaguchi, and Y. Takano, *Appl. Phys. Lett.* **94**, 012503 (2009).

<sup>9</sup>M. H. Fang, H. M. Pham, B. Qian, T. J. Liu, E. K. Vehstedt, Y. Liu, L. Spinu, and Z. Q. Mao, *Phys. Rev. B* **78**, 224503 (2008).

<sup>10</sup>Y. Qiu, W. Bao, Y. Zhao, C. Broholm, V. Stanev, Z. Tesanovic, Y. C. Gasparovic, S. Chang, J. Hu, B. Qian, M. Fang, and Z. Mao, *Phys. Rev. Lett.* **103**, 067008 (2009).

<sup>11</sup>R. Hu, E. S. Bozin, J. B. Warren, and C. Petrovic, *Phys. Rev. B* **80**, 214514 (2009).

<sup>12</sup>S. Margadonna, Y. Takabayashi, Y. Ohishi, Y. Mizuguchi, Y. Takano, T. Kagayama, T. Nakagawa, M. Takata, and K. Prasrides, *Phys. Rev. B* **80**, 064506 (2009); S. Medvedev, T. M. McQueen, I. A. Troyan, T. Palasyuk, M. I. Eremets, R. J. Cava, S. Naghavi, F. Casper, V. Ksenofontov, G. Wortmann, and C. Felsner, *Nat. Mater.* **8**, 630 (2009).

<sup>13</sup>T. Imai, K. Ahilan, F. L. Ning, T. M. McQueen, and R. J. Cava, *Phys. Rev. Lett.* **102**, 177005 (2009).

<sup>14</sup>H. Kotegawa, S. Masaki, Y. Awai, H. Tou, Y. Mizuguchi, and Y. Takano, *J. Phys. Soc. Jpn.* **77**, 113703 (2008).

<sup>15</sup>R. Khasanov, K. Conder, E. Pomjakushina, A. Amato, C. Baines, Z. Bukowski, J. Karpinski, S. Katrych, H.-H. Klauss, H. Luetkens, A. Shengelaya, and N. D. Zhigadlo, *Phys. Rev. B* **78**, 220510(R) (2008).

<sup>16</sup>J. K. Dong, T. Y. Guan, S. Y. Zhou, X. Qiu, L. Ding, C. Zhang, U. Patel, Z. L. Xiao, and S. Y. Li, *Phys. Rev. B* **80**, 024518 (2009).

<sup>17</sup>L. Malone, J. D. Fletcher, A. Serafin, A. Carrington, N. D. Zhigadlo, Z. Bukowski, S. Katrych, and J. Karpinski, *Phys. Rev. B* **79**, 140501(R) (2009).

<sup>18</sup>K. Hashimoto, T. Shibauchi, T. Kato, K. Ikada, R. Okazaki, H. Shishido, M. Ishikado, H. Kito, A. Iyo, H. Eisaki, S. Shamoto, and Y. Matsuda, *Phys. Rev. Lett.* **102**, 017002 (2009).

<sup>19</sup>K. Hashimoto, T. Shibauchi, S. Kasahara, K. Ikada, S. Tonegawa, T. Kato, R. Okazaki, C. J. van der Beek, M. Konczykowski, H. Takeya, K. Hirata, T. Terashima, and Y. Matsuda, *Phys. Rev. Lett.* **102**, 207001 (2009).

<sup>20</sup>C. Martin, R. T. Gordon, M. A. Tanatar, H. Kim, N. Ni, S. L. Bud'ko, P. C. Canfield, H. Luo, H. H. Wen, Z. Wang, A. B. Vorontsov, V. G. Kogan, and R. Prozorov, *Phys. Rev. B* **80**, 020501(R) (2009).

<sup>21</sup>R. T. Gordon, N. Ni, C. Martin, M. A. Tanatar, M. D. Vannette, H. Kim, G. D. Samolyuk, J. Schmalian, S. Nandi, A. Kreyssig, A. I. Goldman, J. Q. Yan, S. L. Bud'ko, P. C. Canfield, and R. Prozorov, *Phys. Rev. Lett.* **102**, 127004 (2009).

<sup>22</sup>R. T. Gordon, C. Martin, H. Kim, N. Ni, M. A. Tanatar, J. Schmalian, I. I. Mazin, S. L. Bud'ko, P. C. Canfield, and R. Prozorov, *Phys. Rev. B* **79**, 100506(R) (2009).

<sup>23</sup>C. Martin, M. E. Tillman, H. Kim, M. A. Tanatar, S. K. Kim, A. Kreyssig, R. T. Gordon, M. D. Vannette, S. Nandi, V. G. Kogan, S. L. Bud'ko, P. C. Canfield, A. I. Goldman, and R. Prozorov, *Phys. Rev. Lett.* **102**, 247002 (2009).

<sup>24</sup>R. T. Gordon, H. Kim, M. A. Tanatar, R. Prozorov, and V. G. Kogan, *Phys. Rev. B* **81**, 180501(R) (2010).

<sup>25</sup>J. D. Fletcher, A. Serafin, L. Malone, J. G. Analytis, J.-H. Chu, A. S. Erickson, I. R. Fisher, and A. Carrington, *Phys. Rev. Lett.* **102**, 147001 (2009).

<sup>26</sup>K. Hashimoto, M. Yamashita, S. Kasahara, Y. Senshu, N. Nakata, S. Tonegawa, K. Ikada, A. Serafin, A. Carrington, T. Terashima, H. Ikeda, T. Shibauchi, and Y. Matsuda, *arXiv:0907.4399* (unpublished).

<sup>27</sup>R. Prozorov, R. W. Giannetta, A. Carrington, P. Fournier, R. L. Greene, P. Guptasarma, D. G. Hinks, and A. R. Banks, *Appl. Phys. Lett.* **77**, 4202 (2000).

<sup>28</sup>V. G. Kogan, C. Martin, and R. Prozorov, *Phys. Rev. B* **80**, 014507 (2009).

<sup>29</sup>C. T. Van Degrift, *Rev. Sci. Instrum.* **46**, 599 (1975).

<sup>30</sup>R. Prozorov, R. W. Giannetta, A. Carrington, and F. M. Araujo-Moreira, *Phys. Rev. B* **62**, 115 (2000).

<sup>31</sup>R. Prozorov and R. W. Giannetta, *Supercond. Sci. Technol.* **19**, R41 (2006).

<sup>32</sup>J. D. Fletcher, A. Carrington, O. J. Taylor, S. M. Kazakov, and J. Karpinski, *Phys. Rev. Lett.* **95**, 097005 (2005).